PERGAMON

Acta mater. 48 (2000) 911–923

Acta MATERIALIA

www.elsevier.com/locate/actamat

# STRUCTURAL STABILITY OF THE LAVES PHASE $Cr_2Ta$ IN A TWO-PHASE Cr–$Cr_2Ta$ ALLOY

**K. S. KUMAR[1]†, L. PANG[1], C. T. LIU[2], J. HORTON[2] and E. A. KENIK[2]**

[1]Division of Engineering, Brown University, Providence, RI 02912, USA and [2]Metals and Ceramics Division, Oak Ridge National Laboratory, Oak Ridge, TN 37831, USA

*(Received 17 August 1999; accepted 4 October 1999)*

**Abstract**—Detailed microstructural analysis of a two-phase alloy of composition Cr–9.8 at.% Ta and lying in the Cr–$Cr_2Ta$ region of the Cr–Ta binary system confirmed that the existing phase diagram is inaccurate; in the cast and annealed condition (1273 K/24 h), blocky primary $Cr_2Ta$ precipitates were observed although the phase diagram indicates the eutectic composition to be ~13 at.% Ta. The eutectic structure is composed of Cr solid solution and the Laves phase $Cr_2Ta$; the morphology is primarily lamellar although the rod morphology was occasionally observed. The Laves phase eutectic microconstituent exhibits the C14 (2H) hexagonal structure with a low stacking fault (basal faults) density and an average composition corresponding to 28.5 at.% Ta. After a prolonged high-temperature anneal (1573 K/168 h), the morphology breaks down to form discrete particles of $Cr_2Ta$; the C14, C36 and C15 structures were all recognized in this annealed condition, often more than one form being present in a single precipitate. The C15 structure was not twinned but contained some stacking faults on the {111} planes. Composition measurements confirmed that these structural transformations were accompanied by composition changes, the precipitates becoming more Ta-rich as they transitioned from the C14 via the C36 to the C15 phase. These observations are coupled with the results from earlier studies to present a discussion on factors that influence the stability and C14/C36/C15 transformation kinetics. © *2000 Acta Metallurgica Inc. Published by Elsevier Science Ltd. All rights reserved.*

*Keywords:* Intermetallic compounds; Laves phase; Phase transformation; Electron diffraction; Energy dispersive X-ray analysis (EDS)

## 1. INTRODUCTION

Binary alloys that include the chromium-containing Laves phase (i.e. $Cr_2X$) have been the subject of several recent investigations [1–7]. The Laves phase, $Cr_2X$, has a compositional range of existence in the respective binary systems (Cr–X, where X = Ti, Zr, Hf, Nb or Ta) and is in equilibrium with the two terminal solid solutions. In all these systems, the published binary phase diagrams [8] show the Laves phase to exhibit the hexagonal C14 (2H) or C36 (4H) structure at high temperatures and the cubic C15 (3C) structure at lower temperatures. At least in the Cr–Nb, and Cr–Ta systems, the C14-to-C15 transformation is shown to occur through a eutectoid or peritectoid transformation, depending on whether a selected two-phase alloy lies in the Cr solid solution + $Cr_2X$ two-phase region or in the X solid solution + $Cr_2X$ two-phase region. The published Cr–Ta phase diagram shown in Fig. 1 demonstrates some of these features.

Under normal solidification conditions, it is likely that these eutectoid and peritectoid reactions will not go to completion, and in these situations, the C14 structure can be metastably retained in the as-cast microstructure of two-phase alloys. This is indeed the case in two-phase alloys of the type Cr–$Cr_2Hf$ [9] and Cr–$Cr_2Ti$ [5], whereas a twinned C15 structure is observed in as-cast Cr–$Cr_2Nb$ alloys [2–4, 10]. It is not clear why the transformation proceeds to completion so readily in the Cr–Nb alloy but not in the Cr–Ti or Cr–Hf alloy. Further, long-term annealing at elevated temperatures has confirmed the sluggish nature of the metastable C14-to-C15 transformation in the Cr–Ti and Cr–Hf alloys. Likewise, as-cast single-phase $Cr_2Nb$ also exhibits the twinned C15 structure [2], whereas as-cast single-phase $Cr_2Ti$ has been shown to maintain the C14 (or C14 + C36) structure at room temperature [5, 6] and to transform to the C15 form via the C36 structure following extended exposures to 1473 K.

The effect of a third element on the structural stability of the $Cr_2Nb$ Laves phase and on the C14/C36/C15 transformation characteristics has been

† To whom all correspondence should be addressed.

1359-6454/00/$20.00 © 2000 Acta Metallurgica Inc. Published by Elsevier Science Ltd. All rights reserved.
PII: S1359-6454(99)00377-8

recently investigated. Takasugi and Yoshida [11] found that when Mo or Ti was substituted for Nb in single-phase $Cr_2Nb$, the C14 (or C36) structure resulted in addition to the C15 structure in the as-cast condition, which upon extended annealing transformed to a twinned C15 structure. Similar observations were made when W was substituted either for Cr alone, or for Cr and Nb. The hexagonal-to-cubic transformation kinetics at 1673 K appeared to depend on the substitutional species, decreasing in the order Mo, Ti and W. An additional interesting observation that was made was that the boundary between the C14 (or C36) and C15 phase in a ternary Cr–Nb–Mo alloy was incoherent; this prompted the authors to argue that the transformation was one that involved both diffusion and shear. These authors [11] have considered a variety of factors that could affect the thermodynamic stability and kinetics of transformations in these Laves phases but most of the discussion is speculative.

Laves phase transformations are thought to occur by shear, and shear transformation kinetics are believed to be dictated by temperature dependence of dislocation mobility [1]. This may well be the case for the transformation of a metastable C14 structure to the stable C15 structure (often via the C36 structure) upon annealing. However, in two-phase alloys containing the metastable C14 structure, it may be necessary for the composition of the C14 phase to first adjust via diffusion to that necessary to stabilize the C15 structure before it can be sheared into the product phase. If the diffusional requirements are minimal and diffusion is adequately rapid, the metastable C14 structure resulting from the suppression of the eutectoid or peritectoid reaction could perhaps shear to the C15 structure *while cooling down*, making it possible to obtain the latter structure in the as-cast material.

In this paper, we report on the microstructure of the Laves phase in a cast binary two-phase Cr–Ta alloy and how it evolves with subsequent annealing at high temperature. Factors that could influence the C14/C15 transformation are discussed based on these observations and results from earlier studies.

## 2. EXPERIMENTAL PROCEDURE

The alloy used in this investigation (Cr–9.8 at.% Ta) was produced by drop casting into a copper mold after arc melting the constituents. The as-cast Cr–Ta ingot was then annealed at 1273 K/24 h to relieve the stresses. A Cr–Ta specimen was also annealed for 168 h at 1573 K and then character-

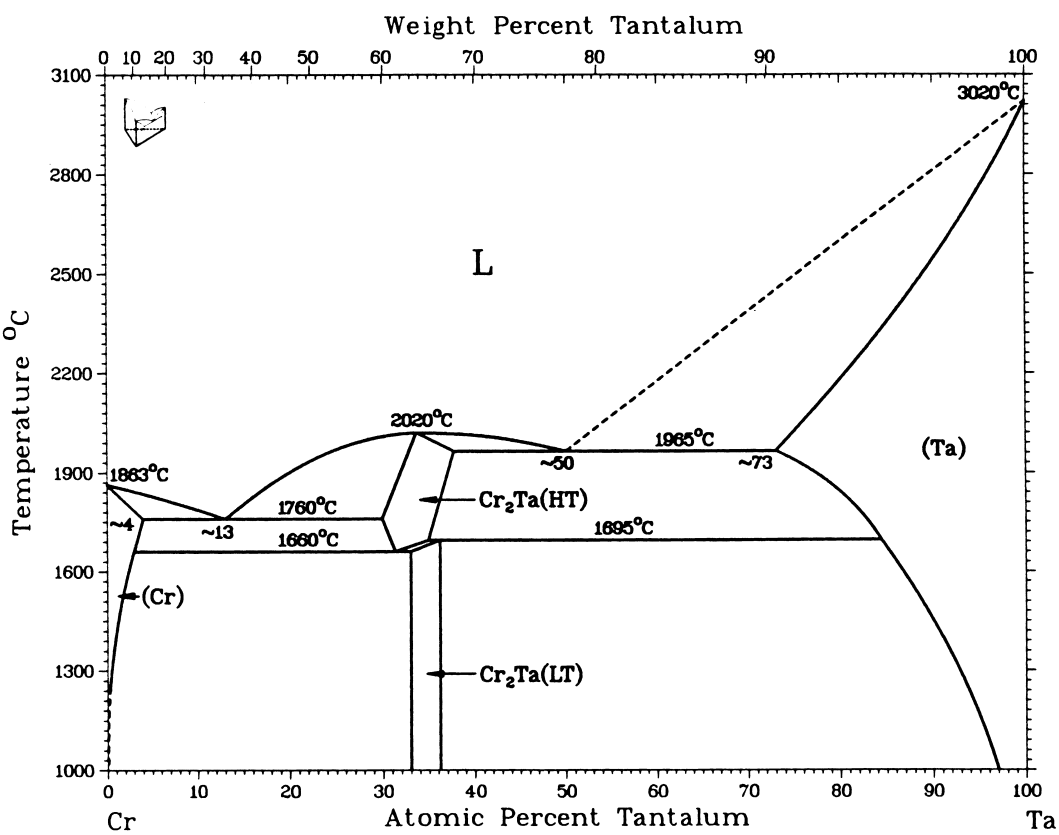


Fig. 1. The binary Cr–Ta phase diagram from Ref. [8].

ized. The microstructure of the alloys was characterized using optical microscopy, scanning electron microscopy (SEM) and transmission electron microscopy (TEM). Thin foil specimens for TEM observations were prepared by slicing sections of appropriate thickness, grinding them down and twin-jet polishing them to perforation using a solution of 10% perchloric acid and 90% methanol at 233 K and 15 V. When adequate electron-transparent area was not obtained using this approach, the perforated foils were further ion-milled for short lengths of time (typically 15–30 min). These specimens were examined using either a JEOL 100CX, a Phillips EM420 or a CM30 (300 kV) transmission electron microscope. Bright field imaging and selected area diffraction (SAD) methods were used to characterize the morphology and crystal structures of the phases present. The compositions of the phases were obtained using energy dispersive X-ray (EDX) techniques in an XL30/FEG SEM and in a CM12 (120 kV) transmission electron microscope. It should be noted that the SEM/EDX quantification was performed using pure Cr AND PURE Ta STANDARDS WHEREAS THE TEM/EDX ANALYSIS WAS STANDARDLESS.

## 3. RESULTS

According to the binary Cr–Ta phase diagram (Fig. 1), alloys whose composition participate in the eutectic reaction $L \Leftrightarrow Cr(\text{solid solution}) + Cr_2Ta$, should produce the C14 phase either only as a eutectic microconstituent (in hypoeutectic alloys) or as a primary phase from the liquid and as a eutectic microconstituent (in hypereutectic alloys). The eutectic microconstituent with the C14 structure (and the primary phase for relevant alloy compositions) must then undergo minor compositional changes (reject Cr with decreasing temperature) before decomposing via a eutectoid reaction at a lower temperature to form a two-phase mixture of Cr solid solution and C15 $Cr_2Ta$. The Cr solid solution in such alloys (primary phase and/or eutectic microconstituent) experiences a decrease in Ta solubility between the eutectic and eutectoid temperatures, and accommodates this decrease in solubility by precipitating C14 $Cr_2Ta$ which also undergoes eutectoid decomposition (with accompanying compositional changes) to produce the C15 $Cr_2Ta$ phase. Since these solid-state reactions involve significant compositional adjustments, it is likely that they will not go to completion under conventional solidification conditions. Further, if the eutectoid temperature is significantly lower than the eutectic temperature and the eutectoid composition is significantly different from the composition of the Laves phase at the eutectic temperature, then the compositional adjustments are even less likely to be accommodated during non-equilibrium freezing. The net result is that it is possible to metastably retain the C14 structure at low temperatures.

The as-cast Cr–9.8 at.% Ta alloy was annealed at 1273 K for 24 h. According to the existing binary phase diagram (Fig. 1), this alloy should correspond to a hypoeutectic composition. Optical microscopy, however, confirmed the microstructure of this alloy to be almost completely eutectic with some isolated coarse primary precipitates [Fig. 2(a)]. Both, lamellar and rod eutectic morphologies were observed. Following the prolonged high-temperature anneal (1573 K/168 h), the lamellar (and rod) morphology breaks down and the precipitates exist as discrete particles [Fig. 2(b)] that are coarser than the average width of the lamellae prior to the high-temperature anneal.

A low-magnification transmission electron micrograph [Fig. 3(a)] confirms the presence of three generations of the $Cr_2Ta$ phase in the cast and 1273 K/24 h annealed specimen: a blocky primary phase with a hexagonal cross-section that was occasionally noted, the lamellar eutectic microconstituent, and solid-state precipitation in the previously denuded

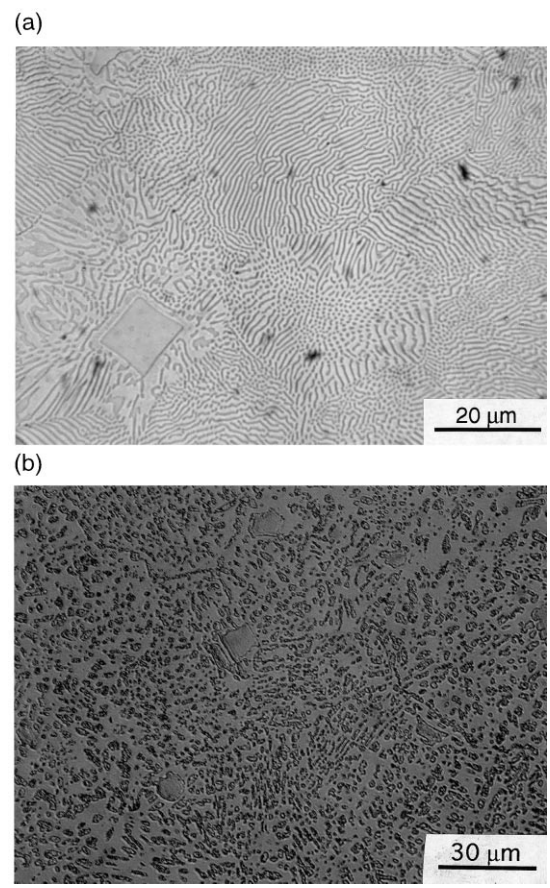


Fig. 2. An optical micrograph of the Cr–9.8Ta alloy: (a) in the cast and annealed condition confirming the presence of primary $Cr_2Ta$ and eutectic $Cr_2Ta$ with rod and lamellar morphology; (b) after annealing for 168 h at 1573 K showing the breakdown of the lamellar structure.

zone between the primary phase and the lamellar eutectic microconstituents. This microstructure is suggestive of an off-eutectic alloy that is marginally hypereutectic. This observation is consistent with the eutectic composition reported by Brady *et al.* [12], but is in conflict with the phase diagram shown in Fig. 1 where the eutectic composition is shown to correspond to ~13 at.% Ta. An examination of the eutectic microstructure at higher magnifications reveals that whereas in some grains, the lamellae are uniform and fairly evenly spaced [Fig. 3(b)], in others, the lamellar morphology breaks down, resulting in faceted rods and rod-to-plate transitions [Fig. 3(c)]. Such transitions in morphology are known to occur as a consequence of local changes in heat-flow patterns and/or composition fluctuations [13, 14]. In some locations where the $Cr_2Ta$ lamellae terminate or form "Y" junctions, the effective spacing between adjacent lamellae changes and in these locations, solid-state precipitation of $Cr_2Ta$ in the Cr solid solution matrix is often noted [Fig. 3(d)]. The composition of the blocky primary Laves phase precipitates was measured using SEM/EDX and, on average, corresponded to 29.7 at.% Ta (Table 1). In contrast, a similar analysis of the eutectic Laves phase microconstituent yielded an average value of 28.5 at.% Ta. This composition is leaner in Ta than that predicted by the phase diagram in Fig. 1. This difference may arise either as a consequence of non-equilibrium cooling of the alloy during drop casting or as a consequence of an inaccurate phase diagram (where the eutectic Laves phase composition is presented as ~30 at.% Ta).

A bright field image of a "Y" junction is shown in Fig. 4(a). This junction is located at the edge of the hole in the specimen. This region (marked X) was used to determine the crystal structure of the $Cr_2Ta$ phase by selected area diffraction. Several zone axes were imaged and six of these are shown in Figs 4(b)–(g). These were consistently indexed to confirm that the $Cr_2Ta$ phase that is a eutectic microconstituent exhibits a hexagonal structure. The relevant portion of a standard (0001) projection for a close-packed hexagonal structure is shown in Fig. 4(h) to illustrate the relationship between the different diffraction patterns shown in Figs 4(b)–(g). When the diffraction patterns are suitably indexed,

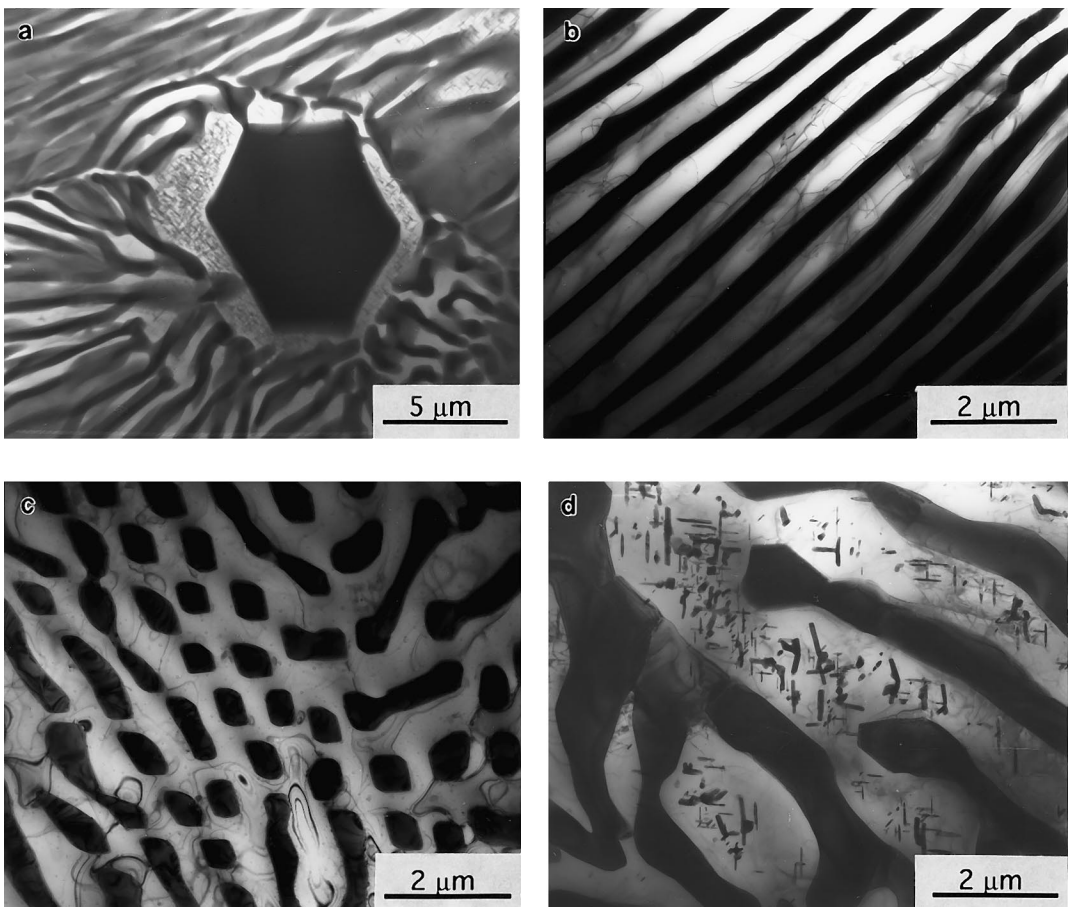


Fig. 3. Bright field images of: (a) primary $Cr_2Ta$ with a precipitate denuded zone that subsequently filled out through solid-state precipitation; (b) lamellar $Cr_2Ta$ eutectic microconstituent; (c) local breakdown of the lamellar morphology; (d) solid-state precipitation of $Cr_2Ta$ between the lamellae.

it is concluded that the $Cr_2Ta$ retains the C14 structure in the cast and annealed (1273 K/24 h) condition. The matrix was confirmed to have the b.c.c. structure expected for Cr solid solution.

A careful examination of some of the $Cr_2Ta$ lamellae at high magnification reveals the presence of several evenly spaced, parallel planar features that exhibit fringe contrast [Fig. 5(a)]. By orienting these features "edge-on" [Fig. 5(b)] and from the associated selected area diffraction pattern corresponding to the $[11\bar{2}0]$ zone axis, we confirm that these features (believed to be stacking faults) lie on the basal plane of the C14 structure. This is analogous to previous observations in the Cr–Hf system [9] and in the Cr–Ti [5] systems where such faults were observed to occur on the basal planes of the C14 structure. The density of such faults on average however appears to be significantly lower in $Cr_2Ta$ as compared to $Cr_2Hf$. Even though the as-cast microstructure was not specifically examined, it is likely that it was composed of Cr solid solution and C14 $Cr_2Ta$ since the C14 structure is still metastably retained following annealing at 1273 K for 24 h.

Following the extended high-temperature anneal (1573 K/168 h), as shown in the optical micrograph in Fig. 2(b), the lamellar structure breaks down completely to yield discrete particles, although the blocky primary precipitates are still present. The average composition of the big blocky primary precipitates after annealing was 30.7 at.% Ta as determined by SEM/EDX (Table 1). Thus, some Ta enrichment (from 29.7% Ta prior to this anneal) of these precipitates is evident as a consequence of the prolonged high-temperature annealing. The discrete particles in the annealed structure resulting from the breakdown of the lamellar structure were also enriched in Ta with an average of 30.4 at.% Ta (compared with 28.5 at.% Ta before the anneal).

The microstructure after the extended high-temperature anneal (1573 K/168 h) was also examined by TEM. A bright field image of one such particle is shown in Fig. 6(a). This particle consists of two distinctly different regions, one of which is heavily faulted (region X) and the other which exhibits a low fault density (region Y). A $[11\bar{2}0]$ SAD pattern [Fig. 6(b)] confirms the region X to have the C36 (4H) hexagonal structure (or a higher order polytype such as 6H) while region Y was found to have the C15 structure as confirmed by the set of diffraction patterns in Figs 6(c)–(e) corresponding to the [101], [121] and [111] zone axes, respectively. A bright field image of another precipitate in the annealed specimen is shown in Fig. 7(a). Here, the two ends of the precipitate (region X for example) are free of stacking faults whereas the central region (region Y) is heavily faulted. A $[11\bar{2}0]$ SAD pattern from region X [Fig. 7(b)] confirms it to have the C14 (2H) hexagonal structure whereas a diffraction pattern from region Y [Fig. 7(c)] shows that this region has the C36 (4H) structure. A bright field image in Fig. 7(d) of a third precipitate shows the presence of multiple variants of stacking faults. This would not be possible for hexagonal structures with basal faults and a set of diffraction patterns corresponding to the [010], [111] and [121] zone axes in Figs 7(e)–(g) confirms this precipitate to have the cubic C15 (3C) structure. Thus it is evident that the 1573 K anneal for 168 h is instrumental in transforming the metastable C14 Laves phase observed in the cast + 1273 K/24 h specimen to C36 and C15 structures.

Since an individual precipitate contained within it regions with different crystal structures (indicative of transformations in progress) and SEM/EDX could not be used to track precipitate composition as a function of crystal structure, we used a standardless EDX technique in the TEM to measure composition within a precipitate as a function of crystal structure. Several individual precipitates were examined; heavily faulted regions, such as region Y in Fig. 7(a) were assumed to correspond to the C36 structures (or higher order polytypes such as a 6H structure) whereas regions containing multiple variants of faults were assumed to be C15 in nature [e.g. Fig. 7(d)]. Those regions that exhibited virtually no faults in the precipitate were thought to be of the C14 type [e.g. region X in Fig. 7(a)]. Although the compositions of the precipitates measured using the EDX attachment in conjunction with the TEM were on average richer in Cr compared with the values obtained using the SEM/EDX (Table 1), an internal comparison of compo-

Table 1. Measured compositions of the Laves phase $Cr_2Ta$ in a binary Cr–9.8 at.% Ta alloy

| Precipitate type | SEM/EDX[a] (at.% Ta) | TEM/EDX[b] (at.% Ta) |
|---|---|---|
| Primary (blocky) precipitate—cast + (1273 K/24 h) anneal | $29.7 \pm 0.4$ | – |
| Primary (blocky) precipitate—after prolonged anneal (1573 K/1 week) | $30.7 \pm 0.1$[c] | – |
| Eutectic $Cr_2Ta$ cast + (1273 K/24 h) anneal | $28.5 \pm 1.2$ | – |
| Globular $Cr_2Ta$ after prolonged anneal (1573 K/1 week) | $30.4 \pm 1.0$ | $25.8 \pm 0.15$ (C14 region[d])[c]<br>$27.3 \pm 0.15$ (C36 region[d])<br>$28.6 \pm 0.8$ (C15 region[d]) |

[a] Pure Cr and pure Ta standards were used.
[b] Standardless analysis.
[c] Only two readings obtained; in all other cases eight to ten readings were obtained.
[d] See text for how these regions were structurally isolated.

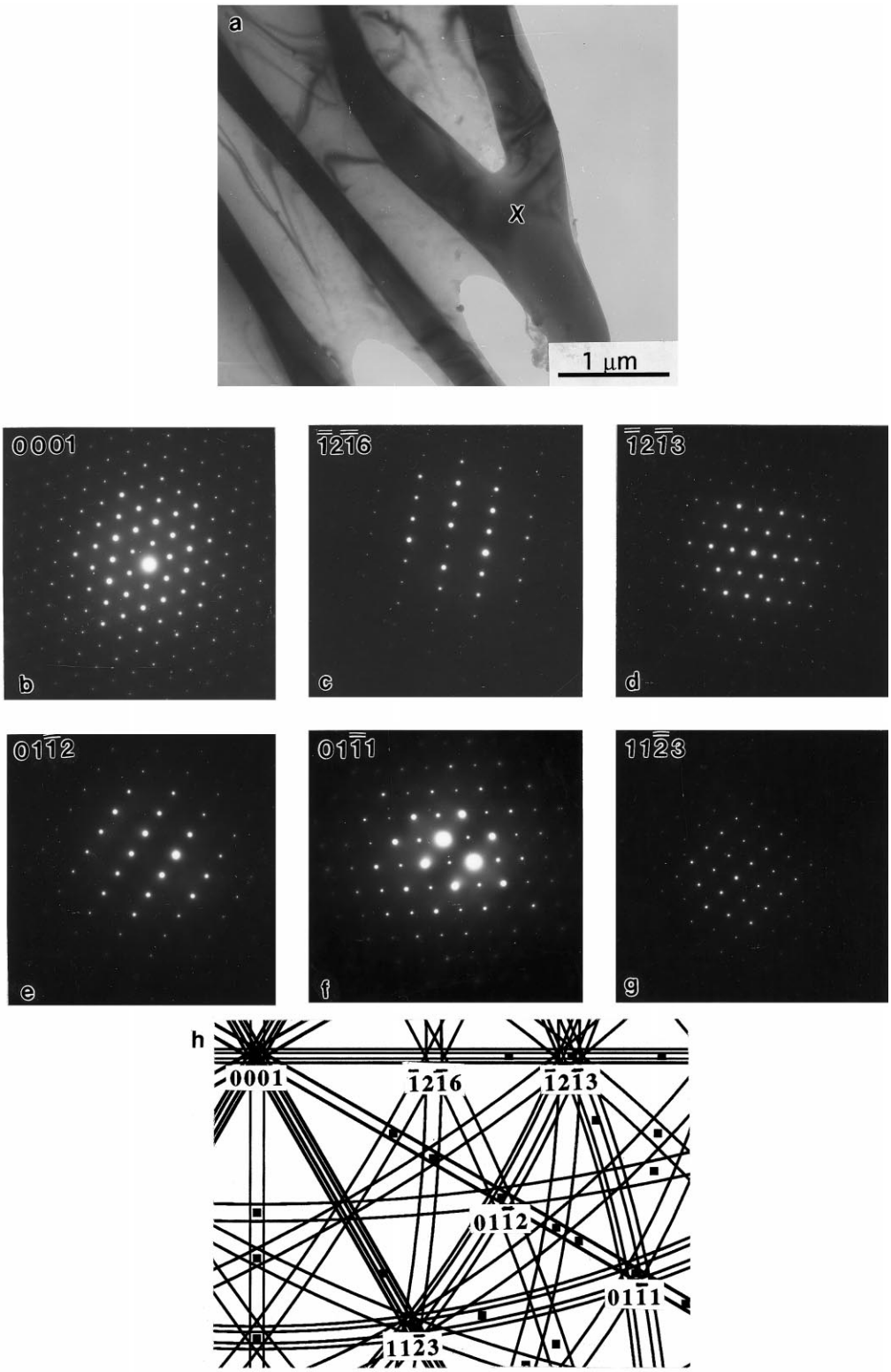


Fig. 4. (a) Bright field image of a "Y" junction in lamellar $Cr_2Ta$ [X marks the location from where selected area patterns (b)–(g) were obtained]; (b)–(g) correspond to [0001], $[\bar{1}2\bar{1}6]$, $[\bar{1}2\bar{1}3]$, $[01\bar{1}2]$, $[01\bar{1}1]$ and $[11\bar{2}3]$ zone axes, respectively. In (h), the relevant portion of a standard (0001) projection is provided to illustrate the relationship between the diffraction patterns shown in (b)–(g).

sition variation with structure could still be made. Thus, regions thought to have the C14 structure, C36 and C15 structures corresponded to average compositions of 25.8, 27.3 and 28.6 at.% Ta, respectively. From these data, it can be seen that the structural transformation from C14 to C15 is accompanied by a gradual increase in Ta content.

## 4. DISCUSSION

Laves phases nominally have the formula $AB_2$ and their occurrence is dictated by the radius ratio of the two components A and B. Frequently, these compounds exhibit a stoichiometric range of existence, with the range being skewed to the smaller atom side and the deviation from stoichiometry being accommodated by anti-site defects [15, 16]. These compounds are known to occur with a hexagonal (C14 and C36) or cubic (C15) structure and the stability regime of the C14, C36 and C15 structures is believed to be governed by the electron concentration-to-atom ratio (e/a). Komura and Kitano [17] have demonstrated this electron concentration dependence of structure in Mg-based binary and ternary Laves phases. More recently, Zhu *et al.* [18] have presented a similar correlation for $Cr_2Nb$-based Laves phases. It is important to recognize however, that such regimes that are identified are empirical and based on structural information collected from existing phase diagrams; their accuracy is therefore limited by the accuracy of the phase diagrams. At elevated temperatures, these compositional regimes may be extended as a consequence of increased solubility, and in fact, Laves phase structures that are not stable at room temperature in some compositional regimes may be present at elevated temperatures. Examples can be seen in the Cr–Nb, Cr–Hf and Cr–Ta phase diagrams where the C14 structure is present at elevated temperature over a compositional range but not at all at lower temperatures. A second feature to note is that in these phase diagrams, at lower temperatures, the C15 structure is stable over a significant compositional range which is not necessarily entirely coincident with the range over which the C14 structure is stable at elevated temperatures, although some compositional overlap exists. However, it should be pointed out that the observed compositions of the C14, C36 and C15 $Cr_2Ta$ in this investigation are consistent with the reported e/a criterion used for predicting the stability regimes of Laves phase types; that is, the decrease in e/a as a consequence of increasing Ta concentration results in the increase in stability of the cubic C15 phase.

A schematic phase diagram that captures the essential features of the Cr–X (X = Nb, Ta and Hf) is shown in Fig. 8. In the Cr–Ti and Cr–Zr systems, a stable C36 phase field is present and

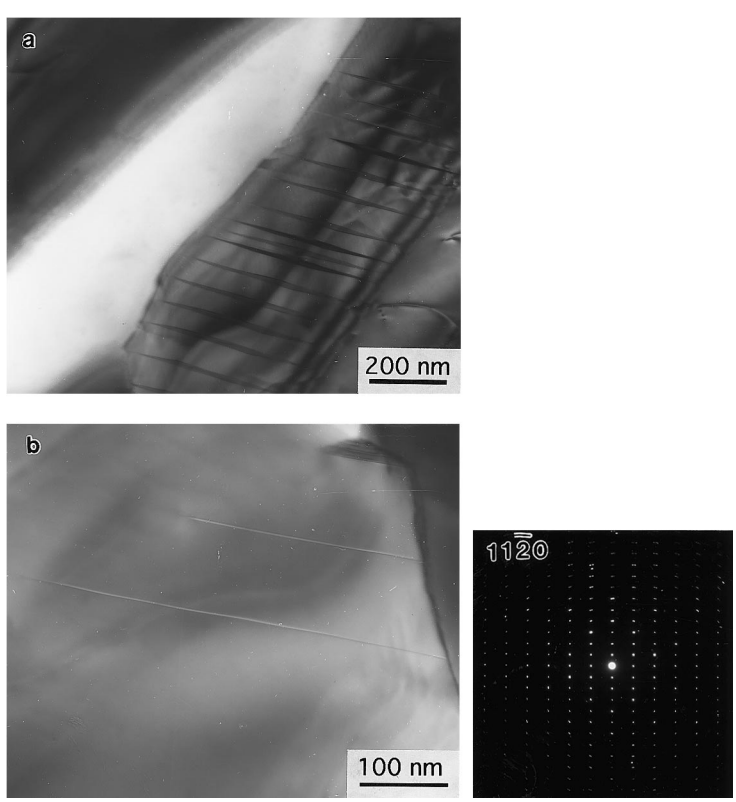


Fig. 5. Bright field images confirming: (a) the presence of planar defects in the lamellar $Cr_2Ta$; (b) that these faults lie on the basal plane in the C14 structure.

for the purpose of clarity, this feature is omitted from Fig. 8. Nevertheless, the following concepts can also be applied to the Cr–Ti and Cr–Zr systems with some modifications. We will use Fig. 8 to develop our discussions on the structural stability and transformation kinetics of Laves phases and draw from our own results and those of others to support some of the arguments.

We can start by considering the alloy compositions that fall within the area "pqsr"; the range

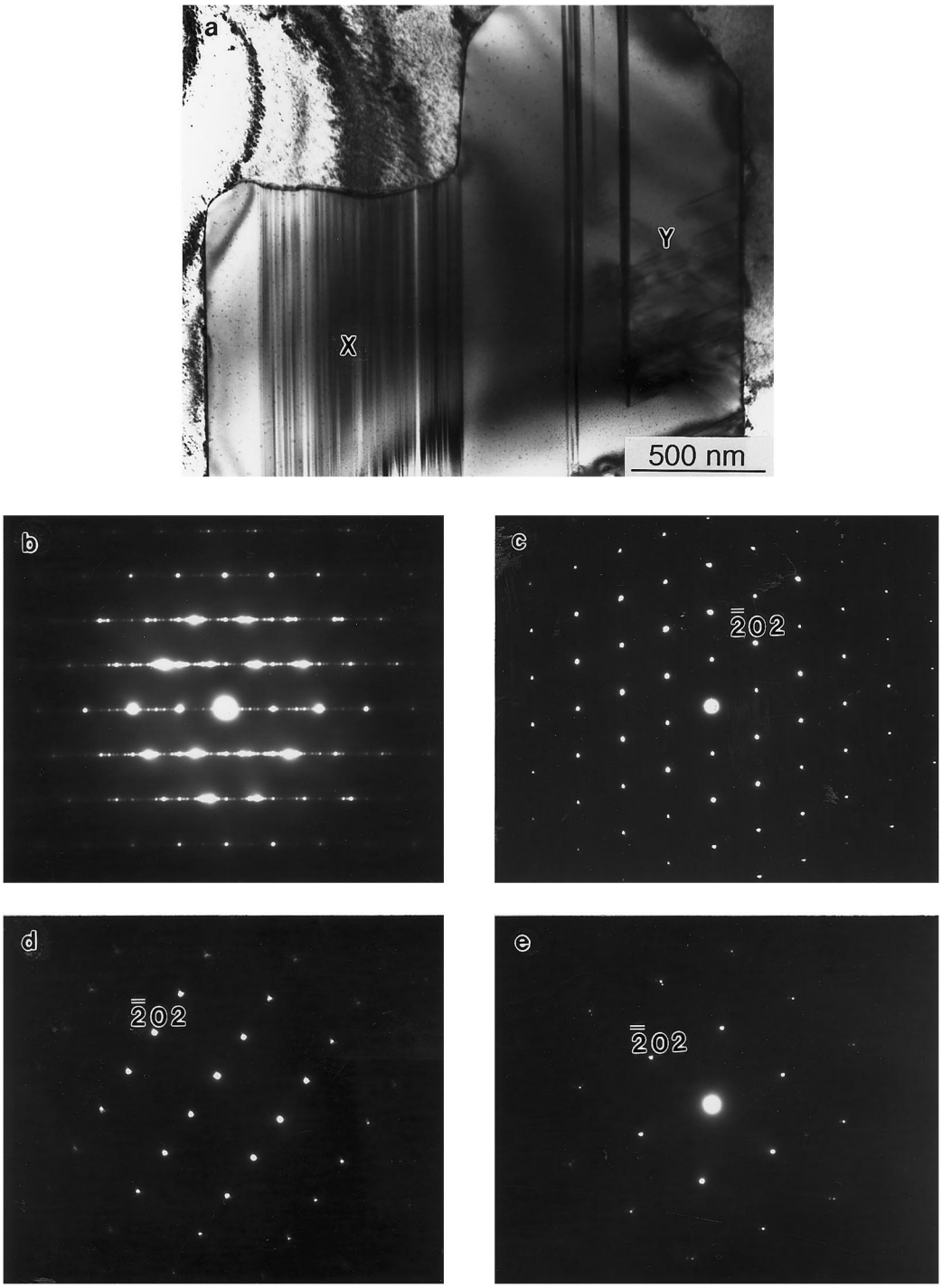


Fig. 6. (a) Bright field image of a discrete Laves phase particle in the Cr–9.8 at.% Ta alloy that was annealed at 1573 K for 168 h showing a heavily faulted region (X) and a region Y containing a low density of faults. Selected area diffraction pattern from region X confirms a hexagonal structure (C36, or a higher order polytype) using the $[11\bar{2}0]$ zone axis, whereas a cubic structure is recognized in region Y using (c) [101], (d) [121] and (e) [111] zone axes.

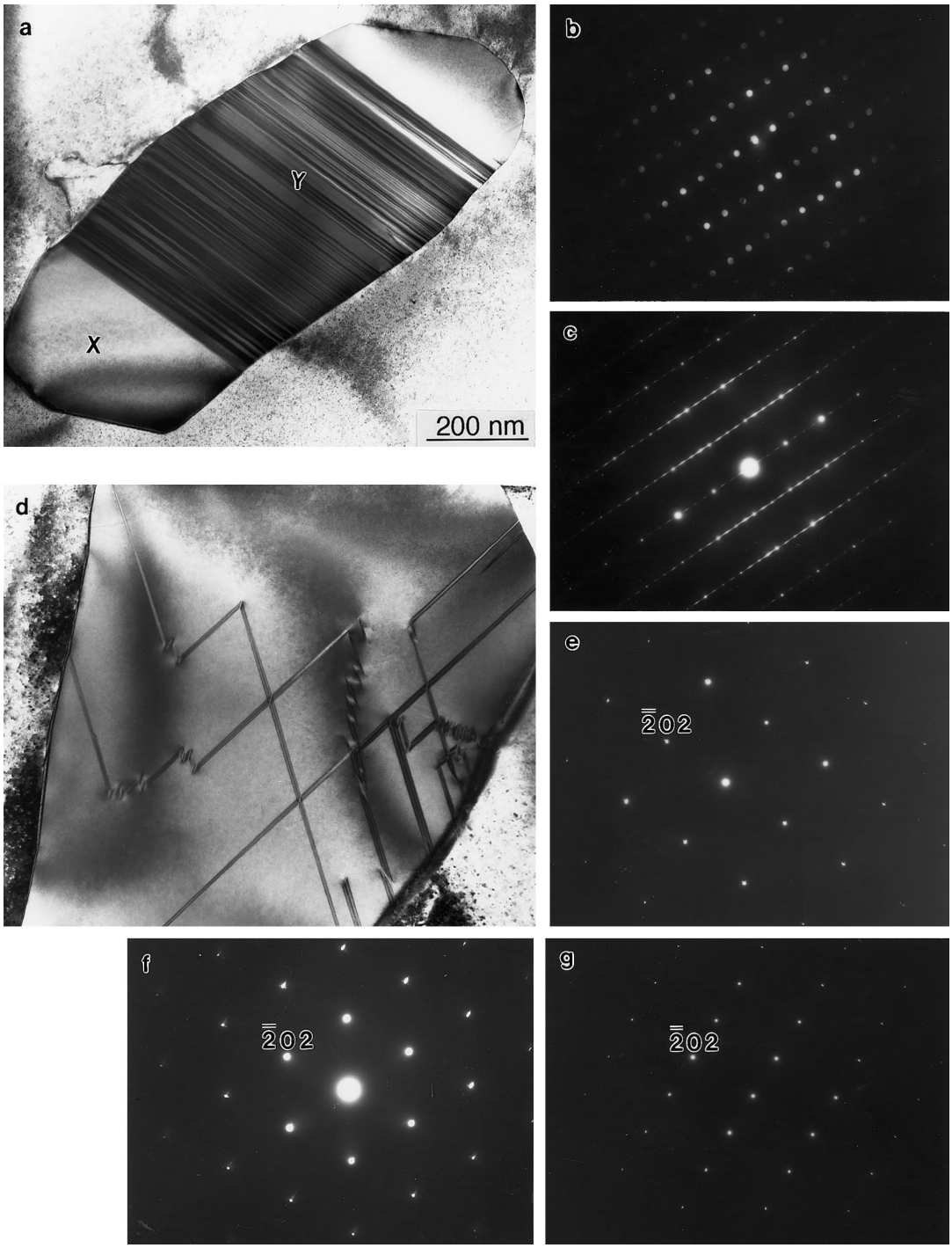


Fig. 7. (a) Bright field of a discrete Laves phase particle in the Cr–9.8 at.% Ta alloy that was annealed at 1573 K for 168 h showing a heavily faulted region (Y) and a region X containing no faults. Selected area diffraction patterns at the $[11\bar{2}0]$ zone axis confirms (b) region X to be C14 and (c) region Y to be C36. (d) A bright field image of another precipitate shows multiple variants of stacking faults on the {111} planes of the cubic C15 structure. Associated diffraction patterns (e)–(g) at the [010], [111] and [121] zone axes, respectively, confirm the cubic structure.

denotes the room temperature composition range for the C15 phase. An alloy composition lying in this range, under equilibrium conditions, will form the C14 structure that upon cooling will transform to the C15 structure through a two-phase region of C14 + C15 where substantial compositional adjustments are required. Such a solid–solid transformation tends to be sluggish and is often suppressed under normal solidification conditions; in addition, in the Cr–Nb and Cr–Ta systems and possibly in the Cr–Hf system, the range of temperature over which the two-phase field is stable for a given composition is small. As cooling continues, the C14 structure is retained metastably but the chemical free energy for forming the C15 structure increases with increased undercooling. Eventually, the C14 structure can shear into the C15 structure often via a metastable intermediate C36 structure [1, 5]. For these alloys, there are no compositional adjustments required for the transformation to proceed and thus it is anticipated that the transformation kinetics will be temperature-dependent to the extent that dislocation mobility in the metastable C14 (and/or C36) phase is affected by temperature [19]. Such a transformation can proceed either during cooling down or subsequently during isothermal annealing. Peculiar to Laves phases is also the fact that synchroshockley dislocation mobility needs to be considered and in this regard, Hazzledine [20] has invoked diffusional requirements at the core of these dislocations for their motion. He has proposed a Zener interchange mechanism at the core in order for the dislocations to move and this is facilitated if vacancies were trapped in the core and a vacancy moved with a kink in the dislocation and enabled the interchange.

For compositions within this range "pqsr", the transformation kinetics is anticipated to vary with composition depending on (1) the slope of the C14 + C15 two-phase region (to a first approximation the slope of the line BC assuming the region to be fairly narrow and bound by straight lines on the top and bottom), (2) the nature of defect structure (such as vacancies) present, and (3) the variation in the intrinsic diffusion coefficients with composition. The second and third factor mentioned above may not be as important for a shear transformation as it would be for a diffusional transformation. For example, in the case of the Cr–Ti system, where the slope of the line BC is steep (B = 1073 K, C = 1493 K over 2 at.% Cr), transformation kinetics has been shown to be a function of stoichiometry [1]. In contrast, in the Cr–Ta and Cr–Nb systems, the slope of the line BC is relatively shallow (B = 1933 K, C = 1968 K over 3 at.% Cr in the Cr–Ta system and B = 1858 K and C = 1898 K over ~7 at.% Cr in the Cr–Nb system [10]) and therefore a substantial difference in transformation kinetics with stoichiometry is not expected. It is worth noting in passing that the eutectoid and peritectoid temperatures are significantly higher in the Cr–Ta and Cr–Nb systems compared with the Cr–Ti and Cr–Hf systems. As mentioned earlier, intrinsic diffusion coefficients can also vary as a function of stoichiometry. Diffusion data on Laves phases are scarce but recently, self-diffusion data for Co and Nb in $Co_2Nb$ in the approximate temperature range 1140–1550 K [21] have been reported. The diffusivity of Nb in $Nb_{31}Co_{69}$ was shown to be considerably slower than that of Co as would be intuitively expected; it was also shown that the diffusivity of Co increased with increasing Co content in the phase. Thus, Co diffusivity in $Nb_{29}Co_{71}$ was found to be significantly higher than in $Nb_{31}Co_{69}$. Thus if the transformation mechanism proposed by Hazzledine [20] is correct, then transformation kinetics at a given temperature may be influenced by stoichiometry as a consequence of diffusion.

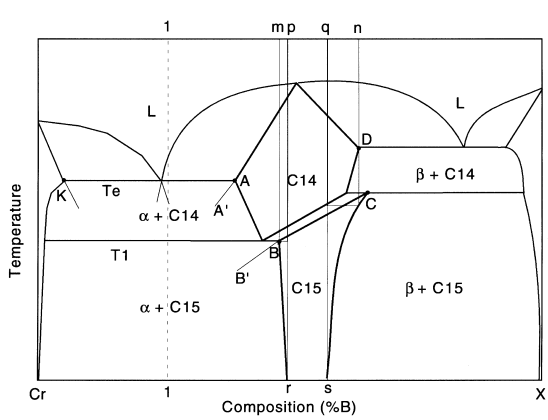


Fig. 8. A schematic Cr–X (X = Nb, Ta, Hf and Zr) phase diagram showing metastable extensions AA′ and BB′. Lines mB, pr, qs and nD denote compositions. The dashed line "1" corresponds to an alloy composition similar to the Cr–9.8 at.% Ta used in this investigation.

Returning to Fig. 8, we next consider transformation from C14 to C15 in those alloys that lie between "mB" and "pr" and between "qs" and "nD". In Fig. 8 we assume that point D is less X-rich than point C (if point D was more X-rich than point C, an additional region between C and D would be present and the situation in that region would be similar to the region between A and B which will be discussed later). Compositions lying in the region bound by "qs" and "nD" and closer to "qs" can metastably retain the C14 structure during non-equilibrium cooling, which can transform by shear into the C15 structure at lower temperatures during cool down without compositional changes provided there is adequate driving force from undercooling. The C15 phase in these alloys will, however, have a non-equilibrium composition at room temperature. For those alloys lying closer to the line "nD" but within the region "qsnD", the C15 phase formation will require minor adjustments

in composition and such adjustments could occur by diffusion at elevated temperatures during cool down. If the appropriate composition that dictates C15 stability at a given temperature is reached and there is simultaneously adequate driving force for the transformation, then shear transformation proceeds and the C15 structure can form. If this does not happen, subsequent isothermal annealing at elevated temperature would produce the required composition change by diffusion and then the structure can shear into the C15 form. Whether these two processes occur simultaneously or sequentially remains to be determined. Similar arguments can be extended for alloys lying in the composition range "mB–pr". It is worth noting that the change in solubility of Cr (or X) with temperature in the C15 Laves phase (i.e. curves Br and sC) influences the transformation response of alloys in these regimes.

Finally, we consider alloy compositions that lie between the compositions corresponding to points A and B in Fig. 8. The analysis presented for this case will also apply to two-phase alloys in the range KA and as typified by alloy 1 marked by dashed lines in Fig. 8. Alloys with compositions lying between points A and B are capable of existing under equilibrium conditions as a single-phase material with the C14 structure at elevated temperatures; a C15 counterpart is however not stable in this composition regime at lower temperatures. Under equilibrium conditions, the phase diagram dictates that such alloys undergo a eutectoid reaction and produce the C15 structure as a eutectoid microconstituent. This requires extensive diffusion and such solid-state reactions involving two substitutional elements are usually sluggish. As a consequence, under normal solidification conditions, it is expected that the C14 structure will be metastably retained at low temperatures. If the composition of point A is fairly close to point B and the eutectoid temperature T1 in Fig. 8 is relatively high, then it is conceivable that minor compositional adjustments can occur during cool down so that a transformed C15 structure is produced in the as-cast alloy, or fairly rapidly upon subsequent isothermal annealing at an elevated temperature. If however, the composition of point A is significantly higher in Cr than that of point B then, extensive diffusion is required for the metastable Laves phase to achieve a composition that is within the structural stability envelope of the C15 structure and consequently, long times at elevated temperatures are required for the transformation to proceed to completion. As mentioned before, these arguments hold equally well for two-phase alloys in the regime defined by KA and of the composition Cr–9.8 at.% Ta studied in this investigation. In considering these two-phase alloys, the metastable C36 structure is frequently encountered as an intermediate product during the transformation of the metastable C14 structure to the stable C15 structure. Metastable solvii for these phase diagrams are not available but it is possible to think in terms of extending the line CB in Fig. 8 to lower temperatures as denoted by the line BB′. In this case, if a two-phase alloy such as alloy 1 that retains the C14 structure to room temperature is isothermally annealed at a temperature below the eutectoid temperature T1 but sufficiently high to permit diffusion to occur in reasonable times, the metastable C14 structure will adjust its composition till it intersects the line BB′ at which point it is capable of transforming to the C15 structure. If a metastable solvus dome is incorporated for the C36 structure that intersects the line BB′ then the intermediate C36 structure will form as the compositional adjustment proceeds before the C15 structure forms. When the required compositional adjustment has occurred, the transformation will proceed by shear. This continuous shift in composition from a Cr-rich C14 structure to a less Cr-rich C15 structure can also be viewed as a progressive change in the e/a ratio which dictates the stability of the various Laves phase polytypes. Finally, it should be noted that while point A provides the equilibrium composition of the eutectic C14 Laves phase microconstituent in two-phase alloys lying in the composition region KA at the eutectic temperature, non-equilibrium freezing processes such as drop casting into a cold copper mold can produce adequate undercooling such that the metastable extension AA′ must be considered to determine the eutectic C14 composition. This implies an even larger deviation in composition that must be adjusted by diffusion during subsequent annealing to permit the C14-to-C15 transformation.

We can now review the results from previous studies as well as from this investigation in light of the above discussion. In the Cr–Nb system, the as-cast *single-phase* alloy ($Cr_2Nb$ phase) exhibits the twinned C15 structure [2]. The C14 structure is still believed to be the stable high-temperature phase but the transformation from the C14 to C15 is thought to be rapid [2] and to proceed during cooling to room temperature. Twinning is thought to be a consequence of the C14-to-C15 transformation. Similar observations have also been made by Takasugi *et al.* [4] in an almost single-phase alloy with the important difference that Bewlay *et al.* [2] made their material by directional solidification at a rate of ~5 mm/min whereas Takasugi *et al.* [4] solidified their "button-melts" on a water-cooled copper hearth. Clearly, the cooling rates in these two cases are different but the transformation nevertheless appears to proceed to completion. In contrast, Thoma and Perepezko [10] reported that in their arc-melted ingot of monolithic $Cr_2Nb$, they observed both, the C14 and C15 phases and implied that the amount of C14 phase that was retained was a function of specimen location in the ingot, being greater in regions that experienced faster

cooling; subsequent annealing, however, produced a single-phase C15 structure.

In the *two-phase* Cr–Nb binary alloys, the as-cast microstructure still consists of the twinned C15 phase. Thoma and Perepezko [10] have reported a composition of $69.17 \pm 0.8$ at.% Cr for the C15 Laves phase in the as arc-melted condition in a Cr–$Cr_2Nb$ two-phase alloy. This is in reasonable agreement with the composition of 70.0 at.% Cr reported by Takeyama and Liu [22] and by Takasugi *et al.* [23]. Following a 100 h anneal at 1673 K, which is a temperature well below the eutectoid temperature, the composition of the C15 phase changes to 68.1 at.% Cr [10]. This implies that for the Cr–Nb phase diagram, the compositions corresponding to points A and B in Fig. 8 are very close to each other. Further, the C14/C15 transformation temperature (the eutectoid temperature) for two-phase Cr–$Cr_2Nb$ alloys in the Cr–Nb system is ~1858 K; it would thus be possible without significant compositional adjustments and the aid of rapid diffusion for the metastable C14 structure to shear into the C15 structure at fairly high temperatures (for example, 50–100 K below the eutectoid temperature). The compositional range of existence of the C15 phase below 1200 K, however, is quite limited compared with the range at ~1750 K. It follows that although enough diffusional adjustments occurred at the elevated temperatures for the C15 structure to be present in the as-cast condition, the composition of the C15 phase still does not correspond to the equilibrium composition at the lower temperatures, and upon subsequent annealing, further compositional adjustments occur. Similar arguments can also be extended to the Nb–$Cr_2Nb$ alloys. In effect, due to the size and shape of the Laves phase fields (composition and temperature regimes) in the Cr–Nb system, the transformation kinetics of two-phase alloys resemble those of the single-phase alloys.

In the Cr–Ti system, *the single-phase* $Cr_2Ti$ composition has been shown to maintain the C14 (or C14 + C36) structure at room temperature and to transform to the C15 form via the C36 structure following extended exposures to 1473 K [5, 6]. The C14/C15 transformation temperature regime for the Cr–Ti system is considerably lower than the corresponding range for the Cr–Nb system. The same argument may also explain the prolonged annealing times required to transform the metastable hexagonal phase to the cubic C15 form, since the annealing temperature must necessarily be below the C14/C15 transformation temperature. The transformation kinetics in the two-phase alloys in the Cr–$Cr_2Ti$ regime as well as the Ti–$Cr_2Ti$ regime are extremely sluggish for similar reasons, with the Ti-rich alloys being somewhat better than the Cr-rich alloys [6].

Transformations in single-phase alloys have not been characterized in the Cr–Ta, Cr–Zr and Cr–Hf systems. The transformation in a two-phase Cr–$Cr_2Hf$ alloy was found to be sluggish with the C14 structure being metastably retained in the as-cast condition and transforming to the C36 structure after extended isothermal annealing; the C15 structure was not observed [9]. The Cr–Hf phase diagram does not appear to be well-developed and therefore it is not possible to discuss the reasons for the sluggish nature of the reaction in the context of compositions and temperatures.

In this study, the composition of the Laves phase eutectic microconstituent in the Cr–9.8 at.% Ta alloy in the cast and annealed (1273 K/24 h) condition corresponds to 28.5 at.% Ta; this is different from the Cr–Nb phase diagram, where the composition of the Laves phase (in the as-cast condition) in two-phase Cr–$Cr_2X$ alloys at the eutectic temperature corresponds to 30.8 at.% Nb. It is interesting to note that after long-term annealing of the Cr–Ta alloy, the average Laves phase composition corresponds to 30.4 at.% Ta which is close to the composition of the $Cr_2Nb$ phase in the Cr–$Cr_2Nb$ two-phase alloys in the as-cast condition. In the Cr–Ta system, in contrast to the Cr–Ti system, the eutectoid temperature is high (1933 K) and this allows isothermal annealing to be performed at high temperatures (e.g. 1573 K/168 h) and consequently, diffusion is fairly rapid and the C14-to-C15 transformation proceeds adequately to evidence the presence of the C15 phase even though the C14 phase has a Cr-rich composition in the reference condition. Composition measurements before and after the prolonged high-temperature anneal (1573 K/168 h) confirm that the C14-to-C15 transformation in the two-phase alloys is accompanied by compositional changes and hence diffusion plays a primary role in affecting transformation kinetics.

## 5. CONCLUSIONS

1. The C14 $Cr_2Ta$ phase is metastably retained as a eutectic microconstituent in a cast and annealed (1273 K/24 h) two-phase Cr–$Cr_2Ta$ alloy. The density of stacking faults in the C14 $Cr_2Ta$ is low, confirming its stability.
2. The observed microstructure in the Cr–Ta alloy confirms that the published Cr–Ta phase diagram is inaccurate in terms of the eutectic composition and the composition of the Laves phase at the eutectic temperature.
3. Following a long-term, high-temperature anneal (1573 K/168 h), the lamellar morphology breaks down and discrete particles of $Cr_2Ta$ are present in a Cr solid solution matrix. These particles were confirmed to be present and exhibited the C14, C36 and C15 structures. Often multiple structures were present in a single particle confirming that they are in the process of transform-

ing from the metastable C14 to the stable C15 structures.

4. The average composition of the Laves phase particles following prolonged high-temperature annealing is richer in Ta compared with the composition of the lamellar eutectic Laves phase microconstituent. This confirms that annealing below the eutectoid temperature leads to the transformation of the C14 structure to more stable configurations and that these transformations are accompanied by compositional changes. Therefore, at least in these two-phase alloys the transformation of the metastable C14 structure to the C36 and C15 structures can be thought of as occurring due to a combination of diffusion and shear. This may in part account for the sluggishness of these transformations.
5. Compositional differences were recognized within individual particles and could be associated with the C14, C36 and C15 structures. Such compositional differences can be thought of in terms of different e/a regimes in which these different structures are stabilized.

*Acknowledgements*—This research was supported by the Division of Materials Science, United States Department of Energy under Contract No. DE-AC05-96OR22464 with Lockheed Martin Energy Research Corporation; L.P. and K.S.K. used the Materials Research Science and Engineering Center (MRSEC) Shared Experimental Facilities at Brown University for a part of this investigation. The MRSEC is supported by the National Science Foundation under Award No. DMR-9632524. Microscopy and microanalysis performed at ORNL was done at the Shared Research Equipment (SHaRE) User Facility.

## REFERENCES

1. Allen, C. W., in *High Temperature Ordered Intermetallic Alloys*, ed. C. C. Koch, C. T. Liu and N. S. Stoloff. Materials Research Society, Pittsburgh, PA, 1985, p. 141.
2. Bewlay, B. P., Sutliff, J. A., Jackson, M. R. and Lipsitt, H. A., *Acta metall. mater.*, 1994, **42**, 2869.
3. Kumar, K. S. and Liu, C. T., *Acta metall. mater.*, 1997, **45**, 3671.
4. Takasugi, T., Yoshida, M. and Hanada, S., *Mater. Sci. Engng*, 1995, **A192–193**, 805.
5. Allen, C. W., Delavignette, P. and Amelinckx, S., *Physica status solidi (a)*, 1972, **9**, 237.
6. Chen, K. C., Allen, S. M. and Livingston, J. D., in *High Temperature Ordered Intermetallic Alloys VI*, Vol. 364, ed. J. Horton, *et al.* Materials Research Society, Pittsburgh, PA, 1995, p. 1401.
7. Liu, C. T., Tortorelli, P. F., Horton, J. A. and Carmichael, C. A., *Mater. Sci. Engng*, 1996, **A214**, 23.
8. Venkatraman, M. and Neumann, J. P., in *Binary Alloy Phase Diagrams*, Vol. 1, ed.-in-chief T. B. Massalski, ed. J. L. Murray, L. H. Bennett and H. Baker. American Society for Metals, Metals Park, OH, 1986, p. 867.
9. Kumar, K. S. and Miracle, D. B., *Intermetallics*, 1994, **2**, 257.
10. Thoma, D. J. and Perepezko, J. H., *Mater. Sci. Engng*, 1992, **A156**, 97.
11. Takasugi, T. and Yoshida, M., *J. Mater. Res.*, 1998, **13**, 2505.
12. Brady, M. P., Zhu, J. H., Liu, C. T., Totorelli, P. F. and Walker, L. R., *Intermetallics*, in press.
13. Hunt, J. D. and Chilton, J. P., *J. Inst. Metals*, 1962–63, **91**, 338.
14. Jackson, K. A. and Hunt, J. D., *Trans. TMS–AIME*, 1966, **236**, 1129.
15. Smith, A. W., Rogers, J. A. and Rawlings, R. D., *Physica status solidi (a)*, 1973, **15**, K119.
16. Bruckner, W., Kleinstuck, K. and Schulze, G. E. R., *Physica status solidi*, 1967, **23**, 475.
17. Komura, Y. and Kitano, Y., *Acta crystallogr.*, 1977, **B33**, 2496.
18. Zhu, J. H., Liaw, P. K. and Liu, C. T., *Mater. Sci. Engng*, 1997, **A239–240**, 260.
19. Kubsch, H., Paufler, P. and Schulze, G. E. R., *Physica status solidi (b)*, 1973, **56**, 231.
20. Hazzledine, P. M., in *Twinning in Advanced Materials*, ed. M. H. Yoo and M. Wuttig. The Minerals, Metals and Materials Society, Warrendale, PA, 1994, p. 403.
21. Denkinger, M., Mehrer, H., in E. P. George, M. J. Mills and M. Yamaguchi. *High Temperature Ordered Intermetallic Alloys VIII*, Vol. 552, ed. E. P. George, M. J. Mills and M. Yamaguchi, 1999. MRS, Warrendale, PA, P. KK 7.6.1.
22. Takeyama, M. and Liu, C. T., *Mater. Sci. Engng*, 1991, **A132**, 61.
23. Takasugi, T., Kumar, K. S., Liu, C. T. and Lee, E. H., *Mater. Sci. Engng*, 1999, **A260**, 108.